SIDEROPHILE ELEMENT ABUNDANCES IN THE Ni-RICH ATAXITES GEBEL KAMIL, DUMONT AND TINNIE. T. J. Campbell[1] and M. Humayun[2], [1]Dept. of Earth, Ocean & Atmospheric Science, and National High Magnetic Field Laboratory, Florida State University, Tallahassee, FL 32310 (tjc08@my.fsu.edu; humayun@magnet.fsu.edu).

Introduction: The recently discovered Ni-rich ataxite Dumont has been grouped with the IVB irons [1]. We have previously reported precise siderophile element abundances on 7 IVB irons and showed that these formed a fractional crystallization sequence with Cape of Good Hope being the earliest solid metal to crystallize from the IVB parental liquid and Warburton Range to be the latest to crystallize [2]. We have recently acquired a number of other IVB irons, particularly Tinnie and Dumont for isotopic studies of correlated Os-W isotope systematics [3]. It is, therefore, important to confirm whether Dumont is a member of the IVB iron group. Both Dumont and Tinnie samples were analyzed for siderophile elements in this study.

The Ni-rich ataxite Gebel Kamil has a Ni content (20.6-20.9% [4]) similar to the IVB irons although its reported composition is too volatile-rich to be considered a member of the IVBs and it remains an ungrouped iron [4]. We included Gebel Kamil in our study to obtain a precise siderophile element composition for this iron.

Analytical Methodology: Polished samples of ~1 cm^2 area were prepared for each of the three irons. Siderophile elements were analyzed using a UP193FX excimer laser ablation system coupled to a Thermo Element XR™ magnetic sector, ICP-MS at the Plasma Analytical Facility at FSU. An area of 800 µm x 500 µm was selected for rastering using a 50 µm beam, scanned at 10 µm/s with the laser firing at 20 Hz and 2.4 GW/cm^2 power. The peaks ^{29}Si, ^{31}P, ^{34}S, ^{51}V, ^{53}Cr, ^{57}Fe, ^{59}Co, ^{60}Ni, ^{63}Cu, ^{66}Zn, ^{69}Ga, ^{74}Ge, ^{75}As, ^{95}Mo, ^{102}Ru, ^{103}Rh, ^{106}Pd, ^{120}Sn, ^{121}Sb, ^{184}W, ^{185}Re, ^{192}Os, ^{193}Ir, ^{195}Pt and ^{197}Au were acquired in low resolution using triple mode detection. Standards used were Hoba IVB iron (Co, Ni, Ru, Rh, Pd, Re, Os, Ir, Pt [5]), North Chile (Filomena) IIA iron (Cu, Ga, Ge, As, W, Au [2]), NIST steel SRM 1263a (V, Cr, Co, Ni, As, Mo, Sn, Sb, W, Au [2]) and NIST SRM 610 glass (Si, P, S, Zn).

Results: The Gebel Kamil sample was analyzed in three areas, each of 800 µm x 500 µm, and the results shown as individual area averages in Table 1, and in Fig. 1, together with a single average and its standard deviation (2σ). Also shown are the abundances reported by [4]. The abundance of P varied from 800-1600 ppm, Cr from 18-23 ppm, Ni from 20.4-20.7 wt %; the abundances of Si, S, and V were below detection limits. Of the siderophile elements, W and Mo showed the largest variability of 9-14% (2σ), while the other siderophile elements varied from 1-4% (2σ) between the three areas of Gebel Kamil, indicating that Gebel Kamil is a very homogeneous iron.

Table 1: Siderophile element abundances in Gebel Kamil, compared with literature sources [4].

	Area 1	*Area 2*	*Area 3*	*Shr.[4]*	*Ind.[4]*
P	780	1610	1100		
V	<1	<1	<1		
Cr	18	23	22		
Fe	786000	782000	783000	786000	783000
Co	7500	7497	7561	7600	7700
Ni	204000	207000	207000	206000	209000
Cu	548	550	548	436	426
Zn	7	6	6		
Ga	53.8	54.8	54.8	49.7	48
Ge	139	141	142	121	116
As	13.1	13.4	13.4	15.6	15.7
Mo	10.4	11.0	11.3	9.9	10
Ru	3.28	3.30	3.32	2.3	2.29
Rh	0.61	0.62	0.61	0.73	0.72
Pd	4.19	4.24	4.21	4.8	4.9
Sn	1.87	1.90	1.85		
Sb	0.265	0.274	0.265	0.28	0.25
W	0.46	0.41	0.40	0.42	0.42
Re	0.040	0.038	0.039	0.04	0.04
Os	0.305	0.302	0.298		
Ir	0.476	0.464	0.459	0.55	0.54
Pt	3.61	3.57	3.53	3.7	3.5
Au	1.53	1.53	1.51	1.57	1.53

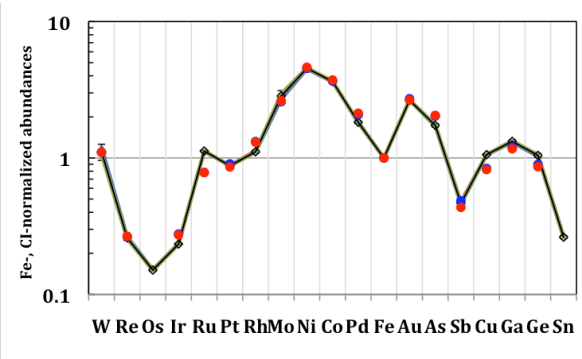

Fig. 1. Fe- and CI-normalized abundances for Gebel Kamil, ungrouped iron. Blue and red dots from [4].

Agreement with data from [4] is excellent, with the largest deviations in the abundances of Cu (21%), Ga (10%), Ge (18%), As (18%), Ru (30%), Rh (18%), Pd

(15%), and Ir (18%). While Gebel Kamil remains an ungrouped iron, its siderophile element abundances place it in the proximity of IAB-IIICD irons [6].

IVB irons: Our new data agree reasonably well with the data of [2], with the exceptions that we have switched our Hoba references values to the more precise dataset of [5] so that there are some discrepancies between the Tinnie and Dumont data collected here and the IVBs reported by [2], particularly for Rh which is now 40% lower than the values of [2]. Fig. 2 shows the new data for Dumont and Tinnie compared with the previous 7 IVBs analyzed by [2].

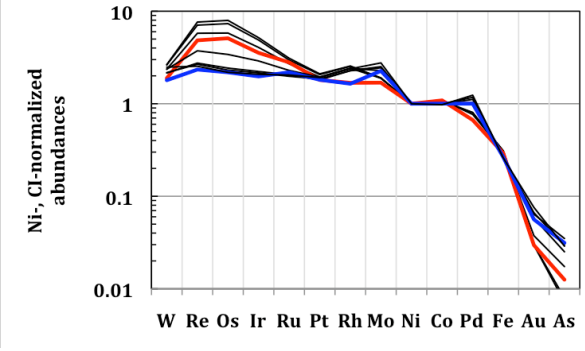

Fig. 2. Dumont (red line) and Tinnie (blue line) siderophile element abundances compared with IVB irons (dark lines [2]).

Crystallization Sequence of IVB irons: Next, we consider the position of Tinnie and Dumont within the crystallization sequence of the IVBs identified by [2]. Tinnie (Ni= 17.75 %) is one of the latest solids to crystallize from the IVB parental liquid, similar to Warburton Range (Ni= 18.02 %). Dumont (Ni= 16.37 %) is similar to Hoba (Ni= 16.33 %) in its position in the crystallization sequence. Tlacotepec and Cape of Good Hope crystallized earlier than Dumont and Hoba.

There ia a rough correlation between the degree of galactic cosmic ray (GCR) neutron capture on the Os and W isotopes in the IVBs and their position in the crystallization sequence. Tinnie, Warburton Range and Weaver Mountains have the most radiogenic W isotopes among the IVBs [3], and all of these are among the latest liquids to crystallize. Tungsten isotopes from Tlacotepec are the most affected by GCR neutron capture [3], and Tlacotepec is one of the earliest solids to crystallize. Tungsten isotopes from Dumont are the next most affected by GCR neutron capture, and Dumont is among the four earliest IVBs in the crystallization sequence. This correlation is approximate only, since most IVBs exhibit a moderate degree of GCR neutron capture on their Os and W isotopes, and this includes Cape of Good Hope and Hoba. Thus, we must consider the relation between position in the crystallization sequence and GCR damage as a suggestive one which may indicate an outside-inwards crystallization with the most shielded irons in the interior of the IVB core. Exhumation of the irons by impacts need not follow a perfectly radial pattern.

References: [1] Weisberg M. et al. (2008) *Meteoritical Bulletin*, *94*, 1551-1558. [2] Campbell A. J. and Humayun M. (2005) *GCA, 69*, 4733-4744. [3] Wittig N. et al. (2012), *LPS, 43*, abstract #1482. [4] D'Orazio M. et al. (2011) *MAPS, 46*, 1179-1196. [5] Walker R. J. et al. (2008) *GCA, 72*, 2198-2216. [6] Wasson J. T. and Kallemeyn G. W. (2002) *GCA, 66*, 2445-2473.